Radio-frequency common-mode noise propagation model for power-line cable

Kamarul, A.; See, Kye Yak; So, Ping Lam; Gunawan, Erry

2005

See, K. Y., So, P. L., Kamarul, A., & Gunawan, E. (2005). Radio-frequency common-mode noise propagation model for power-line cable. IEEE Transactions on Power Delivery. 20(4), 2443-2449.

https://hdl.handle.net/10356/79880

https://doi.org/10.1109/TPWRD.2005.852268

Radio-Frequency Common-Mode Noise Propagation Model for Power-Line Cable

K. Y. See, *Senior Member, IEEE*, P. L. So, *Senior Member, IEEE*, A. Kamarul, and E. Gunawan, *Member, IEEE*

***Abstract*—Electromagnetic-interference (EMI) radiation from a power-line communications (PLC) network has been a major concern for the widespread use of broadband PLC technology. It is also well known that the dominant radiation mode of the PLC network is common mode (CM) by nature. Therefore, for electromagnetic-compatibility planning purposes, knowledge of the CM noise propagation path of the power line in the frequency range of 1 to 30 MHz is essential to provide insight of EMI radiation emitted by the power line. Based on a two-current-probe measurement approach, the CM noise propagation model for a three-wire power-line cable can be derived and represented by an equivalent two-wire CM transmission line. The equivalent CM noise propagation model allows us to predict the CM noise current on the power line with reasonable accuracy. The model will serve as a valuable tool in the future to identify effective ways to suppress EMI radiation from the PLC network.**

***Index Terms*—Broadband communication, electromagnetic compatibility, electromagnetic interference, impedance measurement.**

I. Introduction

THE concept of home networking using broadband power-line communications (PLC) technology is gaining lots of attention in Europe, Asia, and the United States as utilities and telecommunication companies (telcos) seek cost-effective alternatives to bring broadband Internet services to customers. One major concern that prevents the widespread use of broadband PLC systems is the risk of electromagnetic interference (EMI) to radio communications and wireless services [1], [2] caused by their generation of electromagnetic (EM) fields from the power line over which they operate. In recent years, many PLC trials have been performed in various countries to study the feasibility of using the low-voltage power distribution network for fast Internet access as well as to quantify the interference potential at the 1–30 MHz frequency range. The measurement data collected [3], [4] have shown significant levels of radiated emissions from the PLC network.

In recent years, much effort has been put in by several researchers to characterize the radiated emissions associated with PLC networks, ranging from theoretical characterization to experimental assessment. Tests have been performed in [5]–[7] to investigate the relationship between the level of data signals fed into the PLC network and the resulting level of radiated emissions. A transfer function, frequently referred to as a "decoupling factor" [8], [9], has been proposed to define such a relationship. Unfortunately, this method of characterization of EM fields could only provide an estimation of the level of EMI radiation emitted by any arbitrary input signal in the PLC network but was unable to provide further useful information. Although it is well known that the radiation mechanism from the PLC network is common mode (CM) by nature, no comprehensive study has been carried out to characterize and understand the behavior of CM noise current on the PLC network. Such a study is important as it provides essential information to explore possible effective EMI reduction techniques to suppress radiated emissions from the PLC network.

An accurate model of a CM noise propagation path for a power-line cable carrying PLC signals serves as an effective tool to predict the CM noise current on the power-line cable and its associated EM radiation. Although a high-frequency CM noise propagation path of a power-line cable can be derived numerically [10], it requires knowledge of the exact layout geometry of the power-line cable, which is not always possible to obtain, especially for cables embedded in concrete walls. Unlike the differential-mode (DM) noise propagation path, the CM noise propagation path of a power-line cable is more sensitive to its layout geometry and surrounding materials. In addition, numerical modeling techniques can be computationally intensive if they are used to model large PLC networks. In this paper, the CM noise propagation model of a power-line cable is derived from a two-current-probe measurement approach. Since the CM noise propagation model is obtained through measurements, the model derived includes all of the losses of the power-line cables as well as the effects of different layout geometries.

The paper is organized as follows. In Section II, the concept of an equivalent two-wire CM transmission-line model for a three-wire power line cable is introduced. Section III details the theoretical background and the validation of the two-current-probe measurement approach. Section IV is devoted to experimental derivation of the CM noise propagation model of a power-line cable using the proposed measurement approach, and the validation of the model. Section V draws the conclusions.

II. CM Noise Propagation Model

Fig. 1 shows a simple PLC system consisting of a power-line cable and two PLC modems. The CM noise propagating path of the power-line cable could be represented by an electrical model as shown in Fig. 2. For simplicity, it is assumed that only

Manuscript received July 12, 2004; revised August 24, 2004. This work was supported by the Economic Development Board of Singapore. Paper no. TPWRD-00324-2004.

The authors are with Network Technology Research Center, School of Electrical and Electronic Engineering, Nanyang Technological University, Singapore 639798 (e-mail: eplso@ntu.edu.sg).

Digital Object Identifier 10.1109/TPWRD.2005.852268

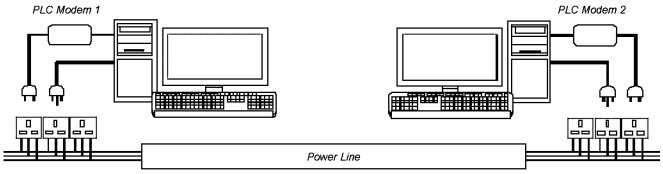

Fig. 1. Simple PLC system.

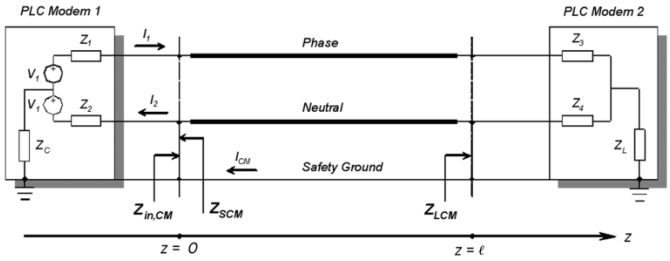

Fig. 2. CM noise propagation path of the PLC system.

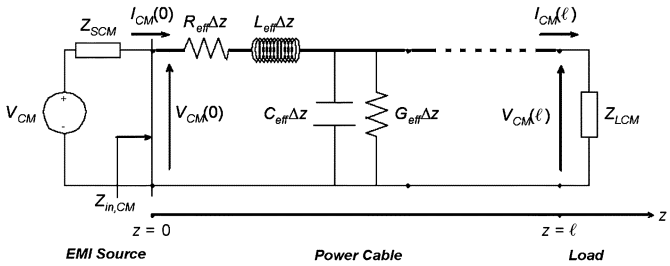

Fig. 3. Two-wire equivalent CM noise propagation model of the power-line cable.

PLC modem 1 transmits a signal with PLC modem 2 acting as a receiver.

The transmitted signals, in the form of DM signals, propagate on an unshielded phase-neutral pair of the power-line cable. However, the electrical unbalances of PLC modem 1 ($Z_1 \neq Z_2$), the pair of wires ($Z_{\mathrm{Phase-Ground}} \neq Z_{\mathrm{Neutral-Ground}}$) and PLC modem 2 ($Z_3 \neq Z_4$), convert a portion of the injected DM signals into unwanted CM signals [11]. Therefore, from the CM noise propagation standpoint, the imbalance of PLC Modem 1 can be modeled as a CM noise source. It is accounted for by a Thevenin equivalent circuit with a CM source voltage V_{CM} and a CM source impedance Z_{SCM}, as shown in Fig. 3.

The imbalance of PLC modem 2 can be represented by its own internal CM impedance Z_{LCM} acting as a CM terminating load. The three-wire power-line cable connecting PLC modems 1 and 2 can be represented by an equivalent two-wire CM transmission line. The thick line is essentially the phase and neutral wires in parallel, and the thin line is the safety ground wire.

$R_{\mathrm{eff}}, L_{\mathrm{eff}}, G_{\mathrm{eff}}$, and C_{eff} are the effective CM resistance per-unit length (in Ω/m), effective CM inductance per-unit length (in H/m), effective CM conductance per-unit length (in S/m), and effective CM capacitance per-unit length (in F/m), respectively. Based on transmission-line theory [12], the CM transmission-line characteristic impedance $Z_{0,\mathrm{CM}}$ and CM propagation coefficient γ can be obtained as

$$\gamma = \alpha + j\beta = \sqrt{(R_{\mathrm{eff}} + j\omega L_{\mathrm{eff}})(G_{\mathrm{eff}} + j\omega C_{\mathrm{eff}})} \quad (1)$$

and

$$Z_{0,\mathrm{CM}} = \sqrt{\frac{R_{\mathrm{eff}} + j\omega L_{\mathrm{eff}}}{G_{\mathrm{eff}} + j\omega C_{\mathrm{eff}}}} \quad (2)$$

where α and β are the effective CM attenuation constant (in Nepers per meter) and phase constant (in radians per meter), respectively. Equations (1) and (2) indicate that γ and $Z_{0,\mathrm{CM}}$ are the characteristic properties of the CM transmission line which are dependent on the values of $R_{\mathrm{eff}}, L_{\mathrm{eff}}, G_{\mathrm{eff}}$ and C_{eff}, and the operating frequency ω, but are independent of the length of the power-line cable.

γ and $Z_{0,\mathrm{CM}}$ can be evaluated by measuring the input impedances of the CM transmission line (at $z = 0$) with the CM load terminals (at $z = \ell$) open-circuited and short-circuited. Using transmission-line theory [12], the CM input impedance of a CM transmission line with a length ℓ and a CM terminating load Z_{LCM} is given by

$$Z_{\mathrm{in,CM}} = Z_{0,\mathrm{CM}} \cdot \frac{Z_{\mathrm{LCM}} + Z_{0,\mathrm{CM}} \tanh(\gamma \cdot \ell)}{Z_{0,\mathrm{CM}} + Z_{\mathrm{LCM}} \tanh(\gamma \cdot \ell)}. \quad (3)$$

If the CM load terminals are short-circuited ($Z_{\mathrm{LCM}} = 0$), (3) becomes

$$Z_{\mathrm{is,CM}} = Z_{0,\mathrm{CM}} \tanh(\gamma \cdot \ell). \quad (4)$$

Similarly, if the CM load terminals are open-circuited ($Z_{\mathrm{LCM}} \to \infty$), (3) becomes

$$Z_{io,\mathrm{CM}} = Z_{0,\mathrm{CM}} \coth(\gamma \cdot \ell). \quad (5)$$

From (4) and (5), we could calculate $Z_{0,\mathrm{CM}}$ and γ

$$Z_{0,\mathrm{CM}} = \sqrt{Z_{io,\mathrm{CM}} \cdot Z_{is,\mathrm{CM}}} \quad (6)$$

$$\gamma = \frac{1}{\ell} \cdot \tanh^{-1} \sqrt{\frac{Z_{is,\mathrm{CM}}}{Z_{io,\mathrm{CM}}}}. \quad (7)$$

Once $Z_{0,\mathrm{CM}}$ and γ are calculated, $R_{\mathrm{eff}}, L_{\mathrm{eff}}, G_{\mathrm{eff}}$, and C_{eff} can be easily obtained by

$$R_{\mathrm{eff}} = \mathrm{Re}(Z_{0,\mathrm{CM}} \cdot \gamma) \quad (8)$$

$$L_{\mathrm{eff}} = \mathrm{Im}\left(\frac{Z_{0,\mathrm{CM}} \cdot \gamma}{\omega}\right) \quad (9)$$

$$G_{\mathrm{eff}} = \mathrm{Re}\left(\frac{\gamma}{Z_{0,\mathrm{CM}}}\right) \quad (10)$$

$$C_{\mathrm{eff}} = \mathrm{Im}\left(\frac{\gamma}{Z_{0,\mathrm{CM}} \cdot \omega}\right). \quad (11)$$

III. Impedance Measurement Using Two-Current-Probe Approach

A. Basic Two-Current-Probe Methodology

An impedance-measuring technique using two clamp-on current probes was originally employed by Nicholson and Malack [13] for DM impedance measurement of ac power distribution in the frequency range of 20 kHz to 30 MHz. Kwasnoik *et al.* [14] extended the frequency range of the measurement method

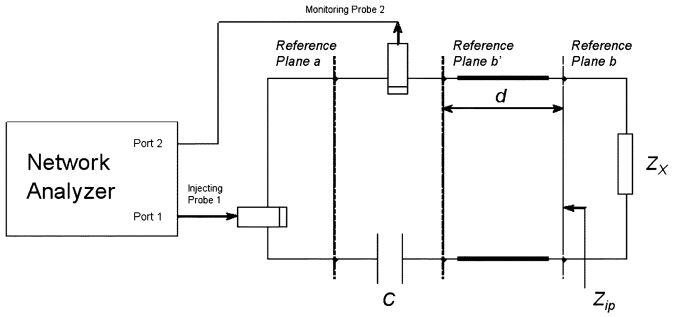

Fig. 4. Two-current-probe measurement methodology.

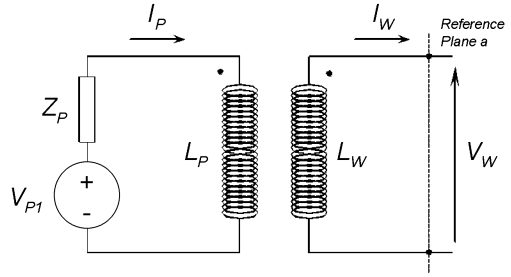

Fig. 5. Equivalent circuit of the injecting current probe.

up to 500 MHz. See and Deng [15] adopted similar measurement method to characterize the CM noise source impedance of a switched-mode power supply in the frequency range of 150 kHz to 30 MHz.

Fig. 4 illustrates the basic setup of the two-current-probe measurement system to measure unknown impedance Z_X. The measurement system consists of two current probes and a network analyzer. The two current probes and a decoupling capacitor C form a high-frequency coupler to avoid direct connection to the ac power mains. A pair of short wires from reference plane b' to reference plane b connects the coupler to Z_X. Port 1 of the network analyzer induces a continuous-wave (CW) signal in the closed loop through the injecting current probe. Port 2 of the network analyzer measures the resultant current in the closed loop with a monitoring current probe.

The injecting current probe can be represented by an equivalent transformer circuit as shown in Fig. 5. V_{p1} is the source voltage, and Z_p is the source impedance of the injecting probe from port 1 of the network analyzer. With the injected signal, the injecting probe induces a voltage V_w and results in a current I_w circulating in the closed loop.

L_p, L_w, and M are the primary self-inductance of the probe, the self-inductance of the wire in the probe volume, and the mutual inductance between the probe and the wire, respectively. V_{p1} and V_w can be expressed as follows:

$$V_{p1} = (Z_p + j\omega L_p)I_p - j\omega M I_w \tag{12}$$

$$V_w = -j\omega M I_p + j\omega L_w I_w. \tag{13}$$

Combining (12) and (13) and eliminating I_p, we have

$$V_w = Z_{M1} I_w - V_{M1} \tag{14}$$

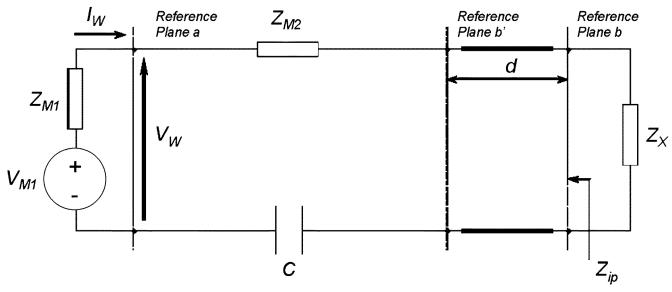

Fig. 6. Equivalent circuit for the two-current-probe setup.

where

$$Z_{M1} = j\omega L_w + \left(\frac{(\omega M)^2}{Z_p + j\omega L_p}\right) \tag{15}$$

$$V_{M1} = V_{p1} \cdot \left(\frac{j\omega M}{Z_p + j\omega L_p}\right). \tag{16}$$

Equations (15) and (16) suggest that the injecting current probe can be represented at reference plane a by a Thevenin equivalent circuit as shown in Fig. 6. Z_{M2} is the reflected impedance in the loop due to the monitoring current probe.

From (16), the ratio V_{M1}/V_{p1}, which is dependent on the probe properties and the operating frequency ω, is given by

$$K_R = \frac{V_{M1}}{V_{p1}} = \frac{j\omega M}{Z_p + j\omega L_p}. \tag{17}$$

If the wire length d between reference planes b' and b is made much shorter than the wavelength of maximum frequency of interest (10 m at 30 MHz), its transmission-line effects can be ignored. Let Z_{ip} be the impedance at the reference plane b as seen by the unknown impedance Z_X. Then

$$V_{M1} = (Z_{ip} + Z_X)I_w \tag{18}$$

where $Z_{ip} = Z_{M1} + Z_{M2} + Z_C$. Substituting V_{M1} from (18) into (17), Z_x can be evaluated by

$$Z_X = (K_R Z_{T2}) \cdot \left(\frac{V_{p1}}{V_{p2}}\right) - Z_{ip} \tag{19}$$

where $Z_{T2} = [V_{p2}/I_w]$ is the transfer impedance of the monitoring current probe. V_{p2} is the voltage received by the monitoring probe. The ratio V_{p1}/V_{p2} can be obtained through S-parameters measurement using the network analyzer as follows:

$$\frac{V_{p1}}{V_{p2}} = \frac{S_{11} + 1}{S_{21}}. \tag{20}$$

The product $K_R Z_{T2}$ is a frequency-dependent coefficient that can be obtained by the following steps: First, remove Z_X and measure Z_{ip} using an impedance analyzer. Then, replace Z_X with a known precision standard resistor R_{std} and measure V_{p2}/V_{p1} again with the network analyzer. Finally, $K_R\, Z_{T2}$ can be obtained by

$$K_R Z_{T2} = \frac{Z_{ip} + Z_{\text{std}}}{\left(\frac{V_{p1}}{V_{p2}}\right)\Big|_{Z_X = Z_{\text{std}}}}. \tag{21}$$

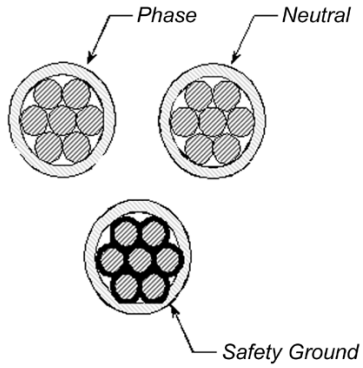

Fig. 7. Cross-sectional view of the in-house power line. The cable used in the measurement has 2.5 mm^2 cross-sectional area, and the diameter of a single copper strand is 0.67 mm.

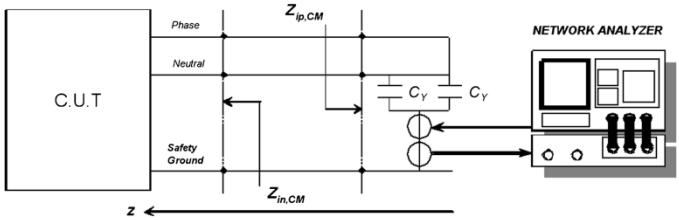

Fig. 8. Two-current-probe setup for measurement of CM input impedance $Z_{\mathrm{in,CM}}$ of cable under test (CUT).

Once $K_R Z_{T2}$ and Z_{ip} are determined, the two-current-probe impedance measurement setup is ready to determine any unknown impedance Z_X using the network analyzer using (19).

B. Validation of Two-Current-Probe Methodology

Tektronic CT-1 (5 mV/mA, 3-dB bandwidth 25 kHz to 1000 MHz) and CT-2 (1 mV/mA, 3 dB bandwidth 1.2 kHz to 700 MHz) current probes are chosen as the injecting and monitoring current probes, respectively. The Agilent 4395A Network Analyzer is employed for the measurement of the S-parameters. To check the accuracy of the two-current-probe measurement method, the following procedure is adopted:

1) Measure Z_{ip} of the measurement setup using an impedance analyzer.
2) Connect the measurement setup to a known standard precision resistor (100 Ω, carbon film ± 1%) and evaluate $K_R Z_{T2}$ using (21).
3) Several standard precision carbon film resistors (270 Ω, 560 Ω, 1.2 kΩ, 2.2 kΩ, and 3.2 kΩ) are selected and each of them is treated as the unknown impedance Z_X and is evaluated using (19).

In general, the differences between measured resistances and stated resistances of these resistors are found to be less than 7% in the frequency range of 1 to 30 MHz.

IV. Experimental Measurements and Results

A. Determination of CM Noise Propagation Path Parameters

The power-line cable under study is a stranded, copper core cable with PVC insulation, as shown in Fig. 7, which is commonly used for in-house wiring. For ease of implementation, the cable under study is not laid in a metal conduit. Fig. 8 shows

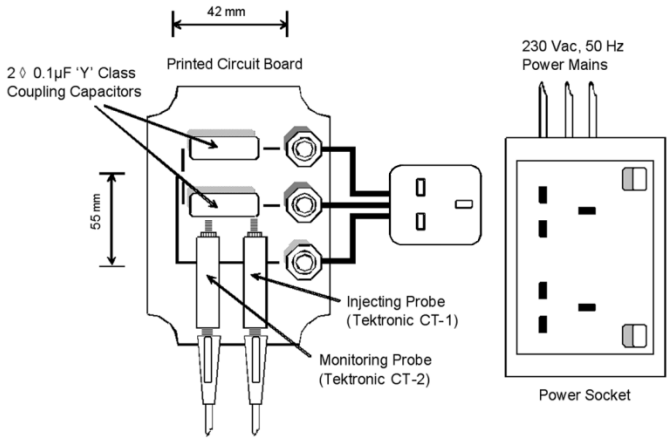

Fig. 9. Implementation of the RF coupling circuit.

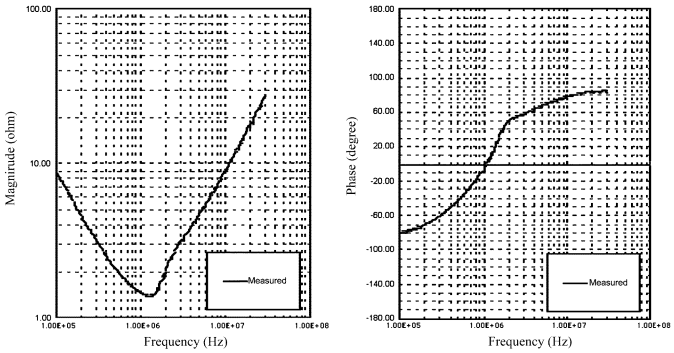

Fig. 10. Measured $Z_{ip,\mathrm{CM}}$ of the RF coupling circuit.

the measurement setup of the CM input impedance of the cable under test (CUT) using the two-current probe approach.

The phase and neutral wires are treated as one single outgoing conductor, and the safety ground wire is the returning conductor. The measurement system consists of two current probes (Tektronic CT-1 and CT-2) and a network analyzer (Agilent 4395A). The two current probes and two coupling 'Y' class 0.1 μF capacitors (one for phase to ground and the other for neutral to ground) form the CM coupling circuit to avoid any direct connection of the analyzer to the ac power mains.

To ensure that the impedance $Z_{ip,\mathrm{CM}}$ of the coupling circuit remains stable and repeatable, the current probes, coupling capacitors, and connecting wires are mounted on a printed-circuit board (PCB) as shown in Fig. 9. The coupling circuit has a rectangular loop area of 42 $\times$ 55 mm. The given loop size is still very much smaller than the wavelength of 30 MHz, our maximum frequency of interest. Therefore, the transmission-line effect of the loop can be safely neglected. $Z_{ip,\mathrm{CM}}$ is measured with the impedance-measuring function of the 4395A network analyzer. Fig. 10 shows the measured $Z_{ip,\mathrm{CM}}$ from 1 to 30 MHz. Based on the measured characteristics of $Z_{ip\mathrm{CM}}$, it can be modeled as a resistor of 1.34 Ω, an inductor of 143 nH, and a capacitor of 0.169 μF in series. With the knowledge of the values of $Z_{ip,\mathrm{CM}}$ of the coupling circuit, and the coefficient K_R Z_{T2} derived earlier, the two-current-probe setup is now ready to measure the unknown CM input impedance of the power-line cable.

The length of the power line under test is 6 m and is mounted at a height of 0.59 m above the concrete floor. The CM input

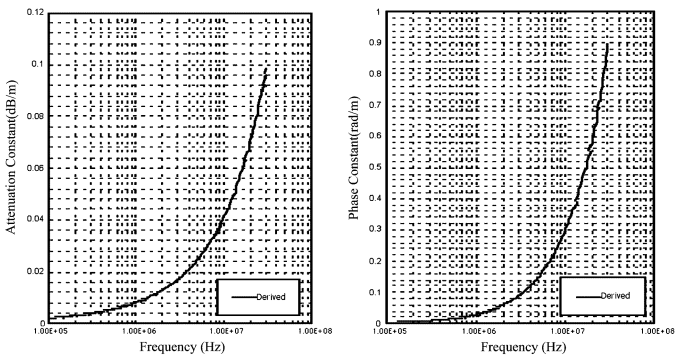

Fig. 11. Derived CM noise propagation constant γ.

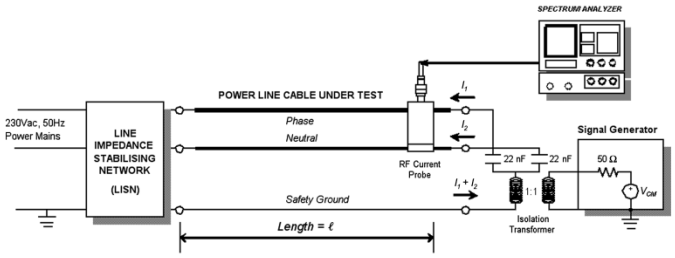

Fig. 12. Setup for verification of the CM noise propagation model.

impedance of the power-line cable is first measured with its load end open-circuited, and then measured again with its load end short-circuited. The CM characteristic impedance $Z_{0,\mathrm{CM}}$ and CM noise propagation constant γ of the power-line cable are evaluated from (6) and (7), respectively. $Z_{0,\mathrm{CM}}$ is found to be at an approximate value of 105 Ω, and the values of γ are shown in Fig. 11. The values of the per-unit length parameters of the CM transmission line $R_{\mathrm{eff}}, L_{\mathrm{eff}}, G_{\mathrm{eff}}$, and C_{eff} are also determined using (8), (9), (10), and (11), respectively. Their values are $R_{\mathrm{eff}} = 0.156\sqrt{f}$ mΩ/m, L_{eff} = 525 nH/m, $G_{\mathrm{eff}} = 4.50f$ pS/m, and $C_{\mathrm{eff}} = 4.75$ pF/m.

B. Verification of CM Noise Propagation Path Model of a Power-Line Cable

The accuracy and reliability of the CM noise propagation path model are verified by comparing the calculated CM current values, which are derived from the model, with the measured CM current values. The power-line cable is driven by a known CM source and terminated with a known CM load, as shown in Fig. 12. The CM source is constructed with two 'Y' class coupling capacitors, an isolating transformer, and a signal generator. The type of power cable used is similar to the one used in the previous experiment as shown in Fig. 7, but with a length of 30 m. The terminating load is the line-impedance stabilization network (LISN) defined by the standards [16], [17]. The LISN provides stabilized impedance (for both phase to ground and neutral to ground) in the frequency range of interest. A Schaffner Chase EMC CSP-8425-1 RF current probe (100-Hz-to-100-MHz bandwidth) is employed to measure CM current on the source end (at $z = 0$) of the power line. This current probe allows measurement of microamp levels of RF current in the presence of high-level power current.

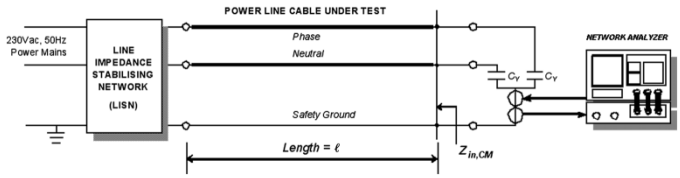

Fig. 13. CM input impedance $Z_{\mathrm{in,CM}}$ measurement setup.

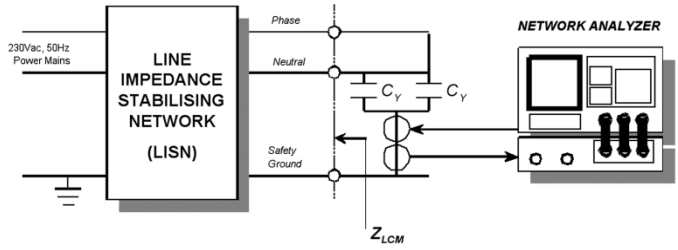

Fig. 14. CM terminating load Z_{LCM} measurement setup.

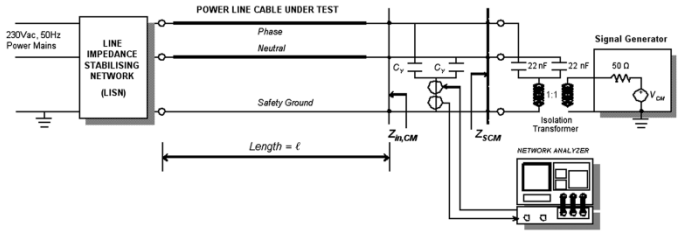

Fig. 15. CM noise source impedance Z_{SCM} measurement setup.

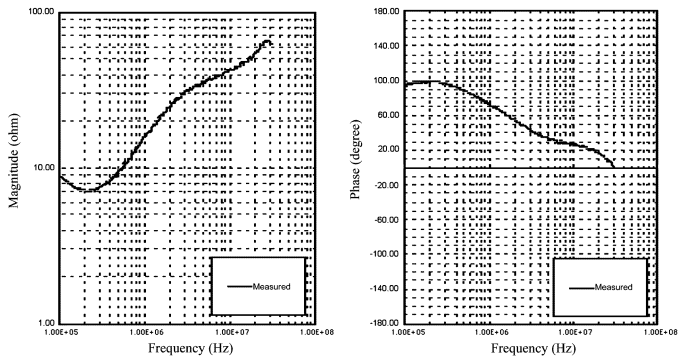

Fig. 16. CM terminating load Z_{LCM}.

The CM input impedance $Z_{\mathrm{in,CM}}$ and CM terminating impedance Z_{LCM} can be measured and obtained easily using the two-current-probe setups as shown in Figs. 13 and 14, respectively. The CM noise source impedance Z_{SCM} can be determined using the two-current-probe setup as shown in Fig. 15. The actual CM impedance measured by the RF coupling circuit is Z_P, which is $Z_{\mathrm{in,CM}}$ and Z_{SCM} in parallel as given by

$$Z_P = \frac{Z_{\mathrm{in,CM}} Z_{\mathrm{SCM}}}{Z_{\mathrm{in,CM}} + Z_{\mathrm{SCM}}}. \tag{22}$$

Since we have determined $Z_{\mathrm{in,CM}}$ and Z_P in the early experiments, we can obtain Z_{SCM} using (22). Figs. 16 and 17 show the values of Z_{LCM} and Z_{SCM}, respectively, which are obtained using the two-current-probe impedance measurement approach.

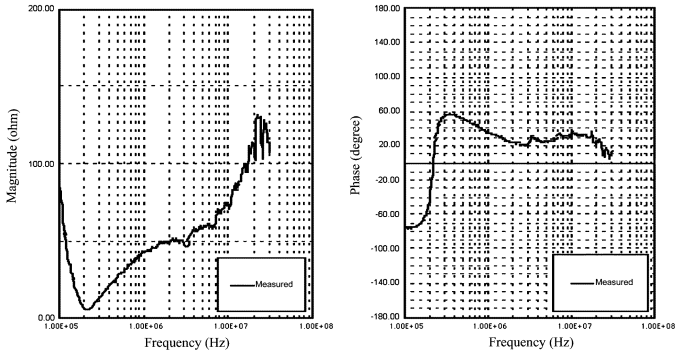

Fig. 17. CM noise source impedance $Z_{\rm SCM}$.

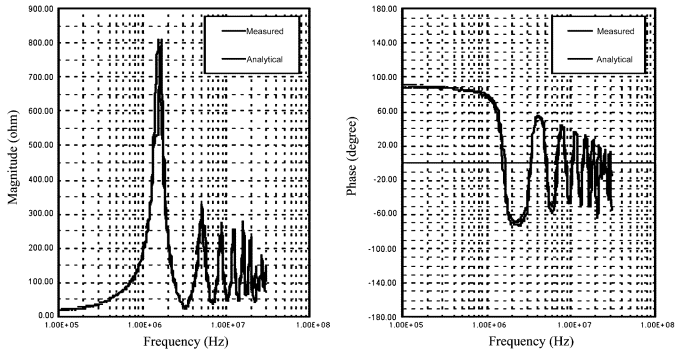

Fig. 18. Comparison of the measured and calculated $Z_{\rm in,CM}$ of the 30-m power line with LISN as the terminating load.

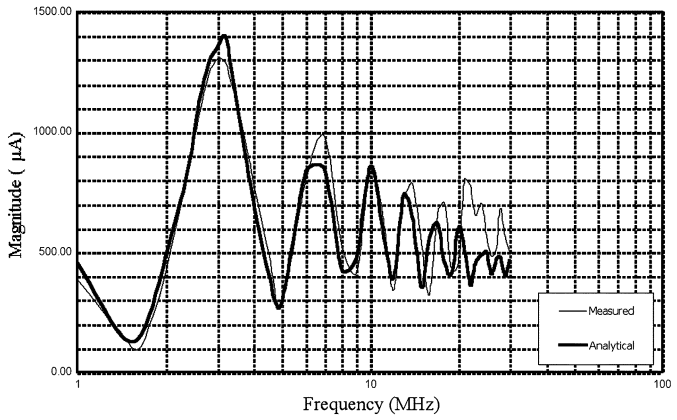

Fig. 19. Comparison of the measured and calculated $I_{\rm CM}$ at the source end of the 30-m power line with 100-mV CM source voltage.

With the knowledge of the CM source impedance $Z_{\rm SCM}$, CM terminating load $Z_{\rm LCM}$, and the previously determined per-unit length parameters of the CM transmission line $R_{\rm eff}, L_{\rm eff}, G_{\rm eff}$, and $C_{\rm eff}$, we can establish a complete CM propagation model for the 30-m power line. Based on the CM propagation model, the input impedance $Z_{\rm in,CM}$ of the terminated power line can be calculated and estimated using (3) by substituting $\ell = 30$ m into the equation. The CM current $I_{\rm CM}$ at the source end of the power-line cable can be evaluated by

$$I_{\rm CM} = \frac{V_{\rm SCM}}{Z_{\rm in,CM} + Z_{\rm SCM}}. \tag{23}$$

Fig. 18 compares the measured and calculated $Z_{\rm in,CM}$. Fig. 19 compares the measured $I_{\rm CM}$ at the source end (at $z = 0$) of the power line using the Schaffner Chase EMC CSP-8425-1 RF current probe and the calculated $I_{\rm CM}$ using (23). Both comparisons demonstrate close agreement between the measured and calculated results.

V. Conclusion

Based on a two-current-probe measurement approach, the RF transmission characteristic of CM noise for any length of power line can be derived. As the distributed per-unit length CM propagation parameters are derived through measurement, the model established includes the losses of the power line as well as factors related to the power-line layout and its surrounding materials. With the knowledge of CM noise propagation model of the power line, the level of the CM current on the power line for different cable lengths and different loading conditions can be estimated with reasonable accuracy. Further work will be carried out to establish the CM noise propagation model of a more complex PLC network that involves multiple interconnecting power lines.

References

[1] S. Roper, "Some issues in the near and far field radiated emission benchmarking of PLT systems," in *Proc. ISPLC Conf.*, 2001, pp. 185–190.

[2] J. M. Silva and B. Whitney, "Evaluation of the potential for power line carrier (PLC) to interfere with use of nation wide differential GPS network," *IEEE Trans. Power Del.*, vol. 17, no. 2, pp. 348–352, Apr. 2002.

[3] C. Muto, N. Mori, and T. Kondoh, "On radio interference assessments of access PLC system," in *Proc. ISPLC Conf.*, 2003, pp. 67–72.

[4] K. Asano, M. Shin, Y. Matsuura, K. Maegawa, S. Yamamoto, and N. Nakayama, "Experimental study of the electromagnetic radiation caused by PLC with high frequency band signals," in *Proc. ISPLC Conf.*, 2004, pp. 143–148.

[5] E. Marthe, F. Rachidi, M. Ianoz, and P. Zweiacker, "Indoor radiated emission associated with power line communication systems," in *Proc. IEEE Int. Symp. Electromagnetic Compatibility*, vol. 1, 2001, pp. 517–520.

[6] C. Hensen and S. Schwarze, "Electromagnetic compatibility for power-line communications on the medium voltage power grid," in *Proc. ISPLC Conf.*, 2001, pp. 155–160.

[7] R. Vick, "Radiated emission caused by in-house PLC-systems," in *Proc. ISPLC Conf.*, 2001, pp. 197–202.

[8] K. Dostert, "EMC aspects of high speed power line communications," in *Proc. Int. Wroclaw Symp. Exhibition Electromagnetic Compatibility*, 2000, pp. 98–102.

[9] M. D'Amore and M. S. Sarto, "Electromagnetic field radiated from broadband signal transmission on power line carrier channels," *IEEE Trans. Power Del.*, vol. 12, no. 2, pp. 624–631, Apr. 1997.

[10] S. A. Pignari and A. Orlandi, "Long-cable effects on conducted emissions levels," *IEEE Trans. Electromagn. Compat.*, vol. 45, no. 1, pp. 43–53, Feb. 2003.

[11] R. M. van Maurick, "Potential common mode currents on the ISDN S and T-interface caused by cable unbalance," in *Proc. IEEE Int. Conf. Electromagnetic Compatibility*, 1992, pp. 202–206.

[12] D. M. Pozar, *Microwave Engineering*, 2nd ed. New York: Wiley, 1998, pp. 56–103.

[13] J. R. Nicholson and J. A. Malack, "RF impedance of power-lines and line impedance stabilization networks in conducted interference measurements," *IEEE Trans. Electromagn. Compat.*, vol. EMC-15, no. 2, pp. 84–86, May 1973.

[14] P. J. Kwasnoik, M. D. Bui, A. J. Kozlowski, and S. S. Stuchly, "Technique for measurement of powerline impedances in the frequency range from 500 kHz to 500 MHz," *IEEE Trans. Electromagn. Compat.*, vol. 35, no. 1, pp. 87–90, Feb. 1993.

[15] K. Y. See and J. Deng, "Measurement of noise source impedance of SMPS using a two probes approach," *IEEE Trans. Power Electron.*, vol. 19, no. 3, pp. 862–868, May 2004.

[16] Federal Communications Commission, *FCC Methods of Measurement of Radio Noise Emissions From Computing Devices*. Washington, DC: FCC, 1987. FCC/OST MP-4.

[17] CISPR Publication, *Information Technology Equipment–Radio Disturbance Characteristics–Limits and Methods of Measurement*, 3rd ed. London, U.K.: CISPR, 1997, vol. CISPR 22.

K. Y. See (SM'02) received the B.Eng. degree (Hons.) in electrical engineering from the National University of Singapore in 1986 and the Ph.D. degree in electrical engineering from Imperial College, London, U.K., in 1997.

Currently, he is an Associate Professor in the School of Electrical and Electronic Engineering, Nanyang Technological University, Singapore. Previously, he was Head of the Electromagnetic Compatibility (EMC) Centre, Singapore Technologies Electronic and Lead EMC Design Engineer with ASTEC Custom Power, Singapore. His research interests are computational electromagnetics, electromagnetic-compatibility (EMC) design for power electronics, signal integrity issues for high-speed design, and EMC measurement techniques.

Dr. See is a Chairman of the IEEE Singapore EMC Chapter, a member of Singapore Technical Committee of EMC, and an active Laboratory Assessor of the Singapore Accreditation Council.

P. L. So (M'98–SM'03) received the B.Eng. degree (Hons.) in electrical engineering from the University of Warwick, U.K., in 1993, and the Ph.D. degree in electrical power systems from Imperial College, University of London, London, U.K., in 1997.

He was a General Assistant Engineer with China Light and Power Company Ltd., Hong Kong, in 1980 and was a Second Engineer working in the field of power system protection until 1991.

Currently, he is an Assistant Professor in the School of Electrical and Electronic Engineering, Nanyang Technological University, Singapore. His research interests are power system dynamics, stability and control, flexible ac transmission systems (FACTS), power quality, and power-line communications.

A. Kamarul received the B.Eng. degree in electrical and electronic engineering from Nanyang Technological University, Singapore, in 2003.

Currently, he is undergoing a Research & Training Programme with The Network Technology Research Center, School of Electrical and Electronic Engineering, Nanyang Technological University, Singapore, under the sponsorship of the Economic Development Board of Singapore in the field of optics. His research interests are in the areas of optical and power-line communications and power-line EMI/EMC issues.

E. Gunawan (M'90) received the B.Sc. degree in electrical and electronic engineering from the University of Leeds, Leeds, U.K., in 1983 and the M.B.A. and Ph.D. degrees from Bradford University, U.K., in 1984 and 1988, respectively.

Currently, he is an Associate Professor with the School of Electrical and Electronic Engineering, Nanyang Technological University, Singapore, where he has been since 1989. From 1984 to 1988, he was a Satellite Communication System Engineer with Communication Systems Research Ltd., Ilkley, U.K. In 1988, he moved to Space Communication (SAT-TEL) Ltd., Northampton, U.K. His research interests are in the fields of digital communications, mobile and satellite communications, error coding, spread-spectrum, and power-line communications. He has published many international research papers and has been a Consultant to local companies on the study of next-generation wireless local-area network (WLAN), digital European cordless telephone (DECT) systems, and Bluetooth.